



HAL
open science

JUNO Physics Prospects

João Pedro Athayde Marcondes de André, Angel Abusleme, Thomas Adam,
Shakeel Ahmad, Rizwan Ahmed, Sebastiano Aiello, Muhammad Akram,
Fengpeng An, Qi An, Giuseppe Andronico, et al.

► **To cite this version:**

João Pedro Athayde Marcondes de André, Angel Abusleme, Thomas Adam, Shakeel Ahmad, Rizwan Ahmed, et al.. JUNO Physics Prospects. 37th International Cosmic Ray Conference (ICRC 2021), Jul 2021, Berlin, Germany. pp.1194, 10.22323/1.395.1194 . hal-03376633

HAL Id: hal-03376633

<https://hal.science/hal-03376633>

Submitted on 13 Oct 2021

HAL is a multi-disciplinary open access archive for the deposit and dissemination of scientific research documents, whether they are published or not. The documents may come from teaching and research institutions in France or abroad, or from public or private research centers.

L'archive ouverte pluridisciplinaire **HAL**, est destinée au dépôt et à la diffusion de documents scientifiques de niveau recherche, publiés ou non, émanant des établissements d'enseignement et de recherche français ou étrangers, des laboratoires publics ou privés.

JUNO Physics Prospects

João Pedro Athayde Marcondes de André^{a,*} on behalf of the JUNO Collaboration
(a complete list of authors can be found at the end of the proceedings)

^a*IPHC, Université de Strasbourg, CNRS/IN2P3, F-67037 Strasbourg, France*

E-mail: jpandre@iphc.cnrs.fr

JUNO is a multi-purpose underground neutrino observatory being constructed in the south of China. The main detector, with a 20 kton liquid scintillator target instrumented with about 18k 20" PMT and about 26k 3" PMT, will be strategically located 53 km from the Taishan and Yangjiang Nuclear Power Plants. Using reactor antineutrinos, JUNO will be able to measure several neutrino oscillation parameters with sub-percent precision as well as to determine the neutrino mass ordering to $\sim 3\sigma$ over 6 years of operation. Furthermore, JUNO will have a broad physics program, ranging from studying neutrinos from other sources, such as solar and supernova neutrinos, to searching for BSM physics such as proton decay. This talk will give an overview on the JUNO's broad physics potential.

37th International Cosmic Ray Conference (ICRC 2021)
July 12th – 23rd, 2021
Online – Berlin, Germany

*Presenter

1. Introduction

Since the discovery of neutrino oscillations at the end of the last century [1, 2] which demonstrated neutrinos are massive particles, significant progress has been made in determining their properties [3]. In order to describe 3 flavor neutrino oscillations, 6 independent parameters are required in total: 2 mass squared differences (Δm_{21}^2 , and Δm_{32}^2 or Δm_{31}^2)¹, 3 mixing angles (θ_{12} , θ_{13} , and θ_{23}), and a CP-violating phase (δ_{CP}). At this moment, most of these parameters have been measured to a $\lesssim 5\%$ precision with the exception of the sign of Δm_{32}^2 and the value of δ_{CP} [4, 5]. The unknown sign of Δm_{32}^2 creates two possible different neutrino mass orderings (NMOs), which are named “normal ordering” (when $m_1 < m_2 < m_3$, with m_i being the mass associated with the neutrino mass eigenstate ν_i) and “inverted ordering” (when $m_3 < m_1 < m_2$). The “inverted” name refers to the fact that in this case the ν_e effective mass is not the smallest, as would have been normally expected given the masses of the other fermions of the Standard Model of Particle Physics.

With the discovery of a rather large θ_{13} value in 2012 [6], it became possible to consider using medium baseline reactor experiments to determine the NMO. The Jiangmen Underground Neutrino Observatory (JUNO) was born of this idea, and then developed to cover a broad physics program including studying neutrinos from natural sources such as solar, supernova, and atmospheric neutrinos, and to search for physics beyond the Standard Model of Particle Physics.

This document relies heavily on Refs. [7, 8]. After an initial description of JUNO in Sec. 2, this proceedings will focus on the NMO measurement in Sec. 3, the precision measurement of oscillation parameters in Sec. 4, and on studies using atmospheric neutrinos in Sec. 5. Studies with JUNO involving supernova neutrinos, the diffuse supernova background, and solar neutrinos are also covered in separate proceedings of this conference [9–11].

2. JUNO

The JUNO detector is located in the south-east of China at a distance of 53 km from the Yangjiang and Taishan Nuclear Power Plants (NPP). This location was selected to optimize the NMO sensitivity using reactor neutrinos, requiring the detector to be placed at the first $\bar{\nu}_e$ disappearance maximum that is driven by Δm_{21}^2 while measuring simultaneously the oscillation pattern from both Δm_{32}^2 and Δm_{21}^2 . JUNO is currently being constructed and is expected to start taking data in 2022.

The JUNO detector is composed of three main parts, as shown in Fig. 1: the Central Detector (CD), the Water Cherenkov Detector (WCD) and the Top Tracker (TT). The CD is composed of a 35.4 m diameter acrylic sphere containing 20 kton of liquid scintillator. This sphere is monitored by 18k 20” and 26k 3” photomultiplier tubes (PMT) that surround the acrylic sphere. High PMT coverage and high light yield liquid scintillator are required for the JUNO CD to reach a 3% energy resolution at 1 MeV, required for the NMO determination. The WCD is a cylinder of diameter 43.5 m and height 44 m surrounding the CD. This volume is filled with 35 kton of ultra-pure water and instrumented with 2.4k 20” PMTs with the goal of tracking atmospheric muons entering the detector and protecting the CD from external radioactivity. The TT, located on top of the WCD,

¹ Δm_{32}^2 and Δm_{31}^2 are not independent as $\Delta m_{31}^2 = \Delta m_{32}^2 + \Delta m_{21}^2$

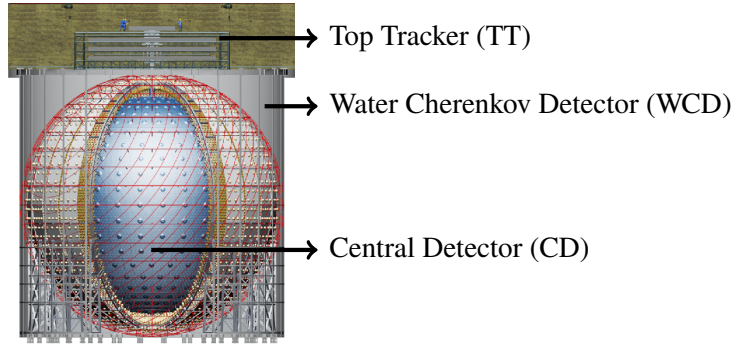


Figure 1: The JUNO detector.

is made of 3 layers of plastic scintillator used to precisely track some of the atmospheric muons entering the detector. The TT covers about 60% of the surface above the WCD.

In JUNO, reactor electron anti-neutrinos will be detected using the inverse beta decay (IBD) reaction: $\bar{\nu}_e + p \rightarrow n + e^+$. The positron produced in this reaction, which will keep most of the electron anti-neutrino energy, will quickly deposit most of its energy and annihilate with electrons in the medium producing a pair of 511 keV gamma-rays. The neutron produced in this reaction, will be captured by a proton after a mean time of about 200 μs , and its de-excitation will produce a 2.2 MeV gamma-ray. The temporal and spatial coincidence signature created by these prompt (positron) and delayed (neutron) signals is characteristic of the IBD and is essential to suppress a large fraction of the background. Given in the IBD the positron keeps most of the neutrino energy, the reconstructed prompt energy is used to determine the electron anti-neutrino energy required for oscillation studies.

Due to the lack of a reference reactor electron anti-neutrino spectrum with a similar resolution to the JUNO detector, the JUNO-TAO detector [12], shown in Fig. 2, was added to the project. The JUNO-TAO detector is located 30 m from one of the Taishan NPP reactor cores. With a surface 10 m^2 of silicon photomultiplier panels operated at -50°C monitoring a 1 ton fiducial volume containing Gd-loaded liquid scintillator, JUNO-TAO will provide an energy spectrum for reactor neutrinos with an energy resolution of less than 2% at 1 MeV which is better than that of JUNO. This reference spectrum will effectively reduce the impact of possible unknown fine-structures in this spectrum [13] on the measurement of neutrino oscillations.

3. Measuring the Neutrino Mass Ordering

The neutrino flux from the Taishan and Yangjiang NPPs will be detected in the JUNO detector as shown in Fig. 3, as a function of the true neutrino energy. In this figure the different oscillation patterns, arising from the Δm_{21}^2 and Δm_{32}^2 oscillation frequencies, can be clearly identified. The slow oscillation, tied to Δm_{21}^2 , shows a single large deficit in the spectrum with a maximum around 3 MeV, but that spans the entire energy range. The fast oscillation, tied to Δm_{32}^2 , produces wiggles in the spectrum over the entire range, but with a much smaller amplitude. The position of these wiggles depends on the neutrino mass ordering and it is through their measurement that JUNO determines the NMO. It is worth noting that in Fig. 3 the true neutrino energy spectra are shown.

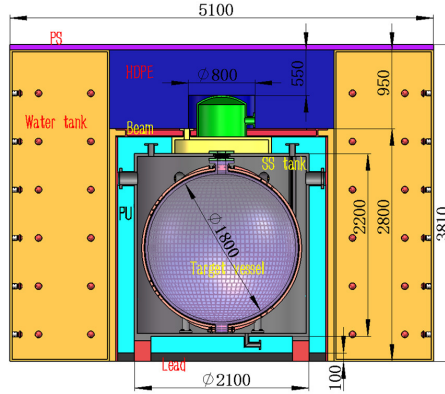


Figure 2: The JUNO-TAO detector.

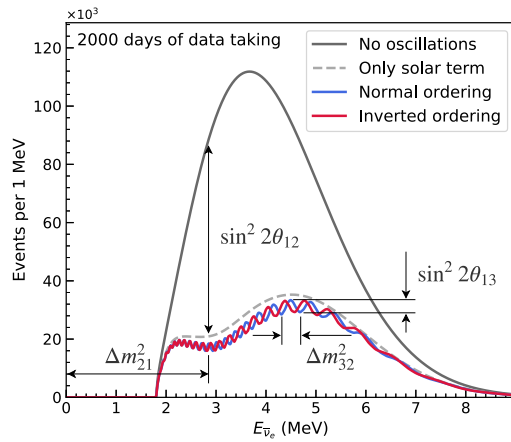


Figure 3: Reactor electron anti-neutrino spectra in JUNO as a function of the neutrino energy. From Ref. [8].

Once the energy resolution of the detector is taken into account the fast wiggles at the lower part of the energy spectrum will no longer be distinguishable, and the measurement will rely mainly on those at higher energies. This is the reason why the detector energy resolution is one of the key parameters towards the measurement of the NMO.

Since Ref. [7], several changes impacted the project with opposing impacts to the NMO analysis [8]. On one hand, only 2 of the 4 originally planned Taishan NPP reactor cores were built. The plans to build the other 2 cores are currently uncertain. On the other hand, the PMT quantum efficiency and the measured light scintillator light yield were higher than considered in Ref. [7]. In addition to these changes, the unoscillated reactor spectrum will now be better constrained than was expected in Ref. [7] thanks to JUNO-TAO. These changes both increase and decrease the JUNO NMO sensitivity and are expected in the end to have a small net impact in the final JUNO sensitivity. Detailed analyses are currently ongoing to provide updated sensitivities, taking into account not only the aforementioned changes but also a more realistic description of the detector and calibration based on measurements done by the collaboration. The discussion on the remainder of this section and on the next section will be done based on Ref. [7].

The sensitivity of JUNO to the NMO is calculated using an Asimov sample. Fits to both

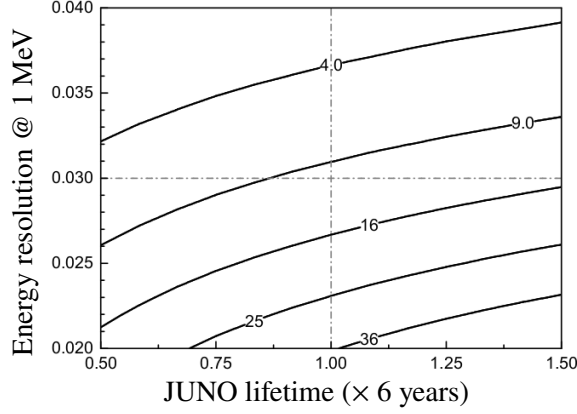


Figure 4: JUNO sensitivity to the NMO ($\Delta\chi^2$ contours) as a function of the JUNO lifetime scaled from 6 years and the energy resolution at 1 MeV. From Ref. [7].

orderings are performed and the difference between minimum χ^2 in the true and false orderings is calculated and noted as $\Delta\chi^2$. For 6 years of data taking, a $\Delta\chi^2 = 16$ is expected considering only statistical errors assuming all reactors cores are located at exactly the same optimal distance of ~ 52.5 km. After taking into account the real distances to each reactor cores² along with adding systematic errors on the signal and background, the JUNO NMO sensitivity is reduced to $\Delta\chi^2 = 10$. In Fig. 4 is shown the dependency of the $\Delta\chi^2$ value obtained as a function of the luminosity, scaled from the 6 years baseline, and the energy resolution at 1 MeV. It highlights the importance of achieving the previously discussed 3% energy resolution as even increasing by 50% the amount of data, JUNO is not able to reach 3σ sensitivity (ie, $\Delta\chi^2 = 9$) for a 3.5% energy resolution. To reach this goal, the JUNO detector uses 4 complementary calibration systems. A detailed calibration strategy for JUNO is presented in Ref. [14], where a $(3.02 \pm 0.01)\%$ energy resolution at 1 MeV and a $(0.03 \pm 0.01)\%$ energy bias are achieved in the baseline detector configuration.

In the previously discussed JUNO sensitivity, no external data is used to constrain the Δm_{32}^2 value fitted by JUNO. By using an external 1% constraint from ν_μ disappearance measurements, the NMO sensitivity can be improved to 4σ [7]. This is possible thanks to the intrinsic difference in the $\bar{\nu}_e \rightarrow \bar{\nu}_e$ and $\nu_\mu \rightarrow \nu_\mu$ oscillations which lead to different best-fit values for Δm_{32}^2 when fitting the wrong ordering. In addition to simply adding a prior from ν_μ disappearance measurements, several analysis performed combining JUNO with accelerator [15] and atmospheric [16–18] neutrino experiments have highlighted the possibility of boosting the NMO sensitivity to 5σ .

4. Precision Measurement of Oscillation Parameters

Using the same sample used for the NMO measurement, it is also possible to determine the values of 4 of the oscillation parameters. The JUNO baseline is ideal for precision measurements of the Δm_{21}^2 and θ_{12} parameters being located in the first $\bar{\nu}_e$ disappearance peak from Δm_{21}^2 . Additionally, the 3% energy resolution will make it possible to measure several Δm_{32}^2 oscillations, enabling JUNO to achieve sub-percent precision on this parameter. While JUNO can also measure θ_{13} , it is

²Including also the Daya-Bay and Huizhou NPP cores which are located at significantly longer baselines.

not expected to achieve the precision of current reactor experiments. Fig. 5 shows JUNO’s expected precision on Δm_{21}^2 , Δm_{ee}^2 , and $\sin^2 \theta_{12}$ as a function of the energy resolution. The Δm_{ee}^2 parameter used in this study is a proxy for Δm_{32}^2 and is defined as: $\Delta m_{ee}^2 = \cos^2 \theta_{12} \Delta m_{31}^2 + \sin^2 \theta_{12} \Delta m_{32}^2$. For the precision measurement of the neutrino oscillation parameters, the energy resolution requirement has a significantly smaller impact, and for all studied energy resolutions JUNO is expected to reach a better than 0.6% precision on these 3 parameters. The changes since Ref. [7] that impacted the NMO analysis will also have an impact in these precision measurements. Taking into account these changes, a reassessment of JUNO’s precision to measure these 3 parameters is in progress, although the results are not expected to change significantly.

5. Atmospheric Neutrinos

As discussed previously, besides measuring reactor neutrinos JUNO will also measure neutrinos from other sources. Among these sources are neutrinos produced in the showers originated by cosmic-rays interacting in the Earth’s atmosphere. Atmospheric neutrinos have a long history of being used to study neutrino oscillations, since their discovery in 1998 by Super-Kamiokande [1]. More recently, atmospheric neutrino experiments have also been proposed to determine the NMO [19, 20] using matter effects during the neutrino propagation through the Earth. While the JUNO detector is not optimized to measure atmospheric neutrinos, the JUNO sensitivity to NMO using atmospheric neutrinos is expected to be between 0.9σ and 1.8σ with 10 years of data, depending on the assumptions regarding the detector capability to identify and reconstruct atmospheric neutrinos [7]. Besides a direct NMO measurement, studies are also ongoing to combine the sensitivity to the NMO using reactor and atmospheric neutrinos within JUNO.

In addition to being used to study neutrino oscillations, JUNO will also be able to measure the $\nu_e + \bar{\nu}_e$ and $\nu_\mu + \bar{\nu}_\mu$ spectrum between 100 MeV and 10 GeV, as shown in Fig. 6. In this analysis, the different hit time patterns of electron and muon neutrinos, caused by the creation of an electron or muon in the neutrino charged current interaction, are used to discriminate the flavor of the detected neutrinos. Given the higher energy of these neutrinos in comparison to reactor neutrinos,

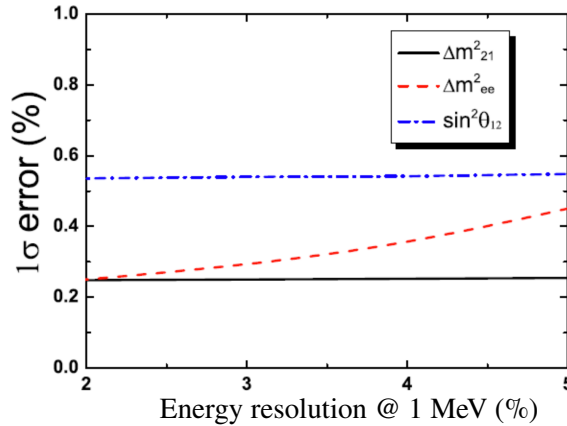


Figure 5: Expected precision on Δm_{21}^2 , Δm_{ee}^2 (used as a proxy for Δm_{32}^2), and $\sin^2 \theta_{12}$ as a function of the energy resolution. From Ref. [7].

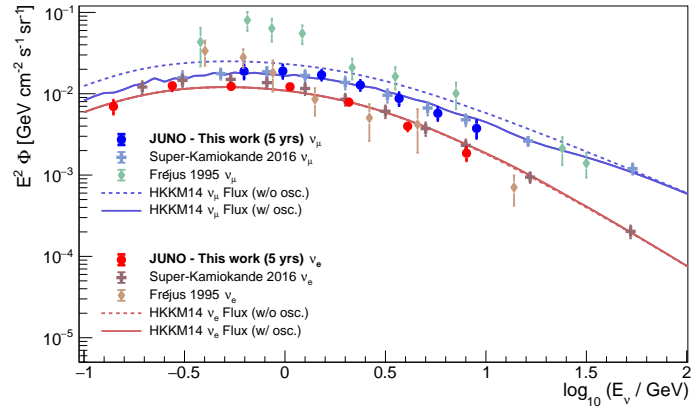


Figure 6: Atmospheric neutrino energy spectra reconstructed for JUNO for ν_μ (blue) and ν_e (red). From Ref. [8].

the 3" PMT system was used primarily to measure these time patterns as its Transit Time Spread of the order of the nanosecond is smaller than that for most 20" PMTs in JUNO. To guarantee a good quality of the energy reconstruction, events close to the detector boundary and partially contained events are rejected. An unfolding method is then used in a Monte Carlo sample to obtain the atmospheric neutrino spectra shown in Fig. 6. The final uncertainties in these unfolded spectra are between 10% and 25% with 5 years of data, showing a great potential of the detector in the atmospheric low energy region. More details about this analysis can be found in Ref. [21].

6. Other Physics Topics in JUNO

In addition to other topics covered in other proceedings in this conference, such as supernova neutrinos [9], diffuse supernova background neutrinos [10], and solar neutrinos [11], JUNO has the potential to address other open questions in a wide range of domains. For example, JUNO will be able to measure the geo-neutrino flux to about 5% precision in 10 years, which can then be compared to the expectation from geological surveys and used to test geological models. In these models, geo-neutrino measurements estimate the abundance of U and Th in the Earth, and, with that, the Earth's heat flow coming from radioactive sources. JUNO will be able to probe Beyond Standard Model physics by looking for nucleon decay, in particular, via the channel $p \rightarrow K^+ + \bar{\nu}$. In this particular channel, JUNO would observe a triple coincidence signature that significantly helps to reject background, and makes it possible for JUNO's sensitivity to reach 8.3×10^{33} years (90% C.L.) with 10 years of data. More details on these studies are available in Refs. [7, 8].

References

- [1] Y. Fukuda et al. (Super-Kamiokande Collaboration). "Evidence for oscillation of atmospheric neutrinos". *Phys. Rev. Lett.*, 81:1562–1567, 1998.
- [2] Q. R. Ahmad et al. (SNO Collaboration). "Direct evidence for neutrino flavor transformation from neutral current interactions in the Sudbury Neutrino Observatory". *Phys. Rev. Lett.*, 89:011301, 2002.

- [3] P. A. Zyla et al. (Particle Data Group Collaboration). “Review of Particle Physics”. *PTEP*, 2020(8):083C01, 2020.
- [4] I. Esteban et al. “The fate of hints: updated global analysis of three-flavor neutrino oscillations”. *JHEP*, 09:178, 2020.
- [5] P. F. de Salas et al. “2020 global reassessment of the neutrino oscillation picture”. *JHEP*, 02:071, 2021.
- [6] F. P. An et al. (Daya Bay Collaboration). “Observation of electron-antineutrino disappearance at Daya Bay”. *Phys. Rev. Lett.*, 108:171803, 2012.
- [7] F. An et al. (JUNO Collaboration). “Neutrino Physics with JUNO”. *J. Phys. G*, 43(3):030401, 2016.
- [8] A. Abusleme et al. (JUNO Collaboration). “JUNO Physics and Detector”. [arXiv:2104.02565](https://arxiv.org/abs/2104.02565), 2021.
- [9] X. Huang (JUNO Collaboration). “Potential of Core-Collapse Supernova Neutrino Detection at JUNO”. [PoS\(ICRC2021\)1076](https://arxiv.org/abs/2104.1076), 2021.
- [10] J. Cheng (JUNO Collaboration). “Diffuse Supernova Neutrino Background Detection at JUNO”. [PoS\(ICRC2021\)1187](https://arxiv.org/abs/2104.1187), 2021.
- [11] J. Zhao (JUNO Collaboration). “Feasibility of detecting B8 solar neutrinos at JUNO”. [PoS\(ICRC2021\)1229](https://arxiv.org/abs/2104.1229), 2021.
- [12] A. Abusleme et al. (JUNO Collaboration). “TAO Conceptual Design Report: A Precision Measurement of the Reactor Antineutrino Spectrum with Sub-percent Energy Resolution”. [arXiv:2005.08745](https://arxiv.org/abs/2005.08745), 2020.
- [13] D. A. Dwyer et al. “Spectral Structure of Electron Antineutrinos from Nuclear Reactors”. *Phys. Rev. Lett.*, 114(1):012502, 2015.
- [14] A. Abusleme et al. (JUNO Collaboration). “Calibration Strategy of the JUNO Experiment”. *JHEP*, 03:004, 2021.
- [15] A. Cabrera et al. “Earliest Resolution to the Neutrino Mass Ordering?”. [arXiv:2008.11280](https://arxiv.org/abs/2008.11280), 2020.
- [16] M. Blennow et al. “Determination of the neutrino mass ordering by combining PINGU and Daya Bay II”. *JHEP*, 09:089, 2013.
- [17] M. Aartsen et al. (JUNO Collaboration members and IceCube Gen2 Collaboration). “Combined sensitivity to the neutrino mass ordering with JUNO, the IceCube Upgrade, and PINGU”. *Phys. Rev. D*, 101(3):032006, 2020.
- [18] J. P. A. M. de André (KM3NeT Collaboration and members of the JUNO Collaboration). “Neutrino mass ordering determination through combined analysis with JUNO and KM3NeT/ORCA”. [PoS\(ICRC2021\)1196](https://arxiv.org/abs/2104.1196), 2021.
- [19] M. G. Aartsen et al. (IceCube-PINGU Collaboration). “Letter of Intent: The Precision IceCube Next Generation Upgrade (PINGU)”. [arXiv:1401.2046](https://arxiv.org/abs/1401.2046), 2014.
- [20] S. Adrian-Martinez et al. (KM3Net Collaboration). “Letter of intent for KM3NeT 2.0”. *J. Phys. G*, 43(8):084001, 2016.
- [21] A. Abusleme et al. (JUNO Collaboration). “Measuring low energy atmospheric neutrino spectra with the JUNO detector”. [arXiv:2103.09908](https://arxiv.org/abs/2103.09908), 2021.

Full Authors List: JUNO Collaboration

Angel Abusleme⁵, Thomas Adam⁴⁵, Shakeel Ahmad⁶⁶, Rizwan Ahmed⁶⁶, Sebastiano Aiello⁵⁵, Muhammad Akram⁶⁶, Fengpeng An²⁹, Qi An²², Giuseppe Andronico⁵⁵, Nikolay Anfimov⁶⁷, Vito Antonelli⁵⁷, Tatiana Antoshkina⁶⁷, Burin Asavapibhop⁷¹, João Pedro Athayde Marcondes de André⁴⁵, Didier Auguste⁴³, Andrej Babic⁷⁰, Nikita Balashov⁶⁷, Wander Baldini⁵⁶, Andrea Barresi⁵⁸, Davide Basilico⁵⁷, Eric Baussan⁴⁵, Marco Bellato⁶⁰, Antonio Bergnoli⁶⁰, Thilo Birkenfeld⁴⁸, Sylvie Blin⁴³, David Blum⁵⁴, Simon Blyth⁴⁰, Anastasia Bolshakova⁶⁷, Mathieu Bongrand⁴⁷, Clément Bordereau^{44,40}, Dominique Breton⁴³, Augusto Brigatti⁵⁷, Riccardo Brugnera⁶¹, Riccardo Bruno⁵⁵, Antonio Budano⁶⁴, Mario Buscemi⁵⁵, Jose Busto⁴⁶, Ilya Butorov⁶⁷, Anatael Cabrera⁴³, Hao Cai³⁴, Xiao Cai¹⁰, Yanke Cai¹⁰, Zhiyan Cai¹⁰, Riccardo Callegari⁶¹, Antonio Cammi⁵⁹, Agustin Campeny⁵, Chuanya Cao¹⁰, Guofu Cao¹⁰, Jun Cao¹⁰, Rossella Caruso⁵⁵, Cédric Cerna⁴⁴, Jinfan Chang¹⁰, Yun Chang³⁹, Pingping Chen¹⁸, Po-An Chen⁴⁰, Shaomin Chen¹³, Xurong Chen²⁶, Yi-Wen Chen³⁸, Yixue Chen¹¹, Yu Chen²⁰, Zhang Chen¹⁰, Jie Cheng¹⁰, Yaping Cheng⁷, Alexey Chetverikov⁶⁷, Davide Chiesa⁵⁸, Pietro Chimenti³, Artem Chukanov⁶⁷, Gérard Claverie⁴⁴, Catia Clementi⁶², Barbara Clerbaux², Selma Conforti Di Lorenzo⁴⁴, Daniele Corti⁶⁰, Flavio Dal Corso⁶⁰, Olivia Dalager⁷⁴, Christophe De La Taille⁴⁴, Jiawei Deng³⁴, Zhi Deng¹³, Ziyang Deng¹⁰, Wilfried Depnering⁵², Marco Diaz⁵, Xuefeng Ding⁵⁷, Yayun Ding¹⁰, Bayu Dirgantara⁷³, Sergey Dmitrievsky⁶⁷, Tadeas Dohnal⁴¹, Dmitry Dolzhikov⁶⁷, Georgy Donchenko⁶⁹, Jianmeng Dong¹³, Evgeny Doroshkevich⁶⁸, Marcos Dracos⁴⁵, Frédéric Druillolle⁴⁴, Ran Du¹⁰, Shuxian Du³⁷, Stefano Dusini⁶⁰, Martin Dvorak⁴¹, Timo Enqvist⁴², Heike Enzmann⁵², Andrea Fabbri⁶⁴, Lukas Faj⁷⁰, Donghua Fan²⁴, Lei Fan¹⁰, Jian Fang¹⁰, Wenxing Fang¹⁰, Marco Fargetta⁵⁵, Dmitry Fedoseev⁶⁷, Vladko Fekete⁷⁰, Li-Cheng Feng³⁸, Qichun Feng²¹, Richard Ford⁵⁷, Amélie Fournier⁴⁴, Haonan Gan³², Feng Gao⁴⁸, Alberto Garfagnini⁶¹, Arsenii Gavrikov⁶¹, Marco Giammarchi⁵⁷, Agnese Giaz⁶¹, Nunzio Giudice⁵⁵, Maxim Gonchar⁶⁷, Guanghua Gong¹³, Hui Gong¹³, Yuri Gornushkin⁶⁷, Alexander Göttel^{50,48}, Marco Grassi⁶¹, Christian Grewing⁵¹, Vasily Gromov⁶⁷, Minghao Gu¹⁰, Xiaofei Gu³⁷, Yu Gu¹⁹, Mengyun Guan¹⁰, Nunzio Guardone⁵⁵, Maria Gul⁶⁶, Cong Guo¹⁰, Jingyuan Guo²⁰, Wanlei Guo¹⁰, Xinheng Guo⁸, Yuhang Guo^{35,50}, Paul Hacksbacher⁵², Caren Hagner⁴⁹, Ran Han⁷, Yang Han²⁰, Muhammad Sohaib Hassan⁶⁶, Miao He¹⁰, Wei He¹⁰, Tobias Heinz⁵⁴, Patrick Hellmuth⁴⁴, Yuekun Heng¹⁰, Rafael Herrera⁵, YuenKeung Hor²⁰, Shaojing Hou¹⁰, Yee Hsiung⁴⁰, Bei-Zhen Hu⁴⁰, Hang Hu²⁰, Jianrun Hu¹⁰, Jun Hu¹⁰, Shouyang Hu⁹, Tao Hu¹⁰, Zhuojun Hu²⁰, Chunhao Huang²⁰, Guihong Huang¹⁰, Hanxiong Huang⁹, Wenhao Huang²⁵, Xin Huang¹⁰, Xingtao Huang²⁵, Yongbo Huang²⁸, Jiaqi Hui³⁰, Lei Huo²¹, Wenju Huo²², Cédric Huss⁴⁴, Safer Hussain⁶⁶, Ara Ioannisian¹, Roberto Isocrate⁶⁰, Beatrice Jelmini⁶¹, Kuo-Lun Jen³⁸, Ignacio Jeria⁵, Xiaolu Ji²⁰, Xingzhao Ji²⁰, Huihui Jia³³, Junji Jia³⁴, Siyu Jian⁹, Di Jiang²², Wei Jiang¹⁰, Xiaoshan Jiang¹⁰, Ruyi Jin¹⁰, Xiaoping Jing¹⁰, Cécile Jollet⁴⁴, Jari Joutsenvaara⁴², Sirichok Jungthawan⁷³, Leonidas Kalousis⁴⁵, Philipp Kampmann⁵⁰, Li Kang¹⁸, Rebin Karaparambil⁴⁷, Narine Kazarian¹, Khanchai Khosonthongkee⁷³, Denis Korablev⁶⁷, Konstantin Kouzakov⁶⁹, Alexey Krasnoperov⁶⁷, Andre Kruth⁵¹, Nikolay Kutovskiy⁶⁷, Pasi Kuusiniemi⁴², Tobias Lachenmaier⁵⁴, Cecilia Landini⁵⁷, Sébastien Leblanc⁴⁴, Victor Lebrin⁴⁷, Frederic Lefevre⁴⁷, Ruiting Lei¹⁸, Rupert Leitner⁴¹, Jason Leung³⁸, Demin Li³⁷, Fei Li¹⁰, Fule Li¹³, Haitao Li²⁰, Huiling Li¹⁰, Jiaqi Li²⁰, Mengzhao Li¹⁰, Min Li¹¹, Nan Li¹⁰, Nan Li¹⁶, Qingjiang Li¹⁶, Ruhui Li¹⁰, Shanfeng Li¹⁸, Tao Li²⁰, Weidong Li^{10,14}, Weiguo Li¹⁰, Xiaomei Li⁹, Xiaonan Li¹⁰, Xinglong Li⁹, Yi Li¹⁸, Yufeng Li¹⁰, Zhaohan Li¹⁰, Zhibing Li²⁰, Ziyuan Li²⁰, Hao Liang⁹, Hao Liang²², Jiajun Liao²⁰, Daniel Liebau⁵¹, Ayut Limphirath⁷³, Sukit Limpijumnon⁷³, Guey-Lin Lin³⁸, Shengxin Lin¹⁸, Tao Lin¹⁰, Jiajie Ling²⁰, Ivano Lippi⁶⁰, Fang Liu¹¹, Haidong Liu³⁷, Hongbang Liu²⁸, Hongjuan Liu²³, Hongtao Liu²⁰, Hui Liu¹⁹, Jianglai Liu^{30,31}, Jinchang Liu¹⁰, Min Liu²³, Qian Liu¹⁴, Qin Liu²², Runxuan Liu^{50,48}, Shuangyu Liu¹⁰, Shubin Liu²², Shulin Liu¹⁰, Xiaowei Liu²⁰, Xiwen Liu²⁸, Yan Liu¹⁰, Yunzhe Liu¹⁰, Alexey Lokhov^{69,68}, Paolo Lombardi⁵⁷, Claudio Lombardo⁵⁵, Kai Loo⁵², Chuan Lu³², Haoqi Lu¹⁰, Jingbin Lu¹⁵, Jinguang Lu¹⁰, Shuxiang Lu³⁷, Xiaoxu Lu¹⁰, Bayarto Lubsandorzhiiev⁶⁸, Sultim Lubsandorzhiiev⁶⁸, Livia Ludhova^{50,48}, Arslan Lukanov⁶⁸, Fengjiao Luo¹⁰, Guang Luo²⁰, Pengwei Luo²⁰, Shu Luo³⁶, Wuming Luo¹⁰, Vladimir Lyashuk⁶⁸, Bangzheng Ma²⁵, Qiumei Ma¹⁰, Si Ma¹⁰, Xiaoyan Ma¹⁰, Xubo Ma¹¹, Jihane Maalmi⁴³, Yury Malyskhin⁶⁷, Roberto Carlos Mandujano⁶⁷, Fabio Mantovani⁵⁶, Francesco Manzali⁶¹, Xin Mao⁷, Yajun Mao¹², Stefano M. Mari⁶⁴, Filippo Marini⁶¹, Sadia Marium⁶⁶, Cristina Martellini⁶⁴, Gisele Martin-Chassard⁴³, Agnese Martini⁶³, Matthias Mayer⁵³, Davit Mayilyan¹, Ints Mednieks⁶⁵, Yue Meng³⁰, Anselmo Meregaglia⁴⁴, Emanuela Meroni⁵⁷, David Meyhöfer⁴⁹, Mauro Mezzetto⁶⁰, Jonathan Miller⁶, Lino Miramonti⁵⁷, Paolo Montini⁶⁴, Michele Montuschi⁵⁶, Axel Müller⁵⁴, Massimiliano Nastasi⁵⁸, Dmitry V. Naumov⁶⁷, Elena Naumova⁶⁷, Diana Navas-Nicolas⁴³, Igor Nemchenok⁶⁷, Minh Thuan Nguyen Thi³⁸, Feipeng Ning¹⁰, Zhe Ning¹⁰, Hiroshi Nunokawa⁴, Lothar Oberauer⁵³, Juan Pedro Ochoa-Ricoux^{74,5}, Alexander Olshevskiy⁶⁷, Domizia Orestano⁶⁴, Fausto Ortica⁶², Rainer Othegeven⁵², Hsiao-Ru Pan⁴⁰, Alessandro Paoloni⁶³, Sergio Parmeggiano⁵⁷, Yatian Pei¹⁰, Nicomede Pelliccia⁶², Anguo Peng²³, Haiping Peng²², Frédéric Perrot⁴⁴, Pierre-Alexandre Petitjean², Fabrizio Petrucci⁶⁴, Oliver Pilarczyk⁵², Luis Felipe Piñeres Rico⁴⁵, Artyom Popov⁶⁹, Pascal Pousset⁴⁵, Wathan Pratunwan⁷³, Ezio Previtali⁵⁸, Fazihi Qi¹⁰, Ming Qi²⁷, Sen Qian¹⁰, Xiaohui Qian¹⁰, Zhen Qian²⁰, Hao Qiao¹², Zhonghua Qin¹⁰, Shoukang Qiu²³, Muhammad Usman Rajput⁶⁶, Gioacchino Ranucci⁵⁷, Neill Raper²⁰, Alessandra Re⁵⁷, Henning Reber⁴⁹, Abdel Rebi⁴⁴, Bin Ren¹⁸, Jie Ren⁹, Barbara Ricci⁵⁶, Markus Robens⁵¹, Mathieu Roche⁴⁴, Narongkiat Rodphai⁷¹, Aldo Romani⁶², Bedřich Roskovec⁴¹, Christian Roth⁵¹, Xiangdong Ruan²⁸, Xichao Ruan⁹, Saroj Rujirawat⁷³, Arseniy Rybnikov⁶⁷, Andrey Sadovsky⁶⁷, Paolo Saggese⁵⁷, Simone Sanfilippo⁶⁴, Anut Sangka⁷², Nuanwan Sanguansak⁷³, Utane Sawangwit⁷², Julia Sawatzki⁵³, Fatma Sawy⁶¹, Michaela Schever^{50,48}, Cédric Schwab⁴⁵, Konstantin Schweizer⁵³, Alexandr Selyunin⁶⁷, Andrea Serafini⁵⁶, Giulio Settanta⁵⁰, Mariangela Settimo⁴⁷, Zhuang Shao³⁵, Vladislav Sharov⁶⁷, Arina Shaydurova⁶⁷, Jingyan Shi¹⁰, Yanan Shi¹⁰, Vitaly Shutov⁶⁷, Andrey Sidorenkov⁶⁸, Fedor Šimkovic⁷⁰, Chiara Sirignano⁶¹, Jaruchit Siripak⁷³, Monica Sisti⁵⁸, Maciej Słupecki⁴², Mikhail Smirnov²⁰, Oleg Smirnov⁶⁷, Thiago Sogo-Bezerra⁴⁷, Sergey Sokolov⁶⁷, Julianan Songwadhana⁷³, Boonrucksar Soonthornthum⁷², Albert Sotnikov⁶⁷, Ondřej Šrámek⁴¹, Wintorn Sreethawong⁷³, Achim Stahl⁴⁸, Luca Stanco⁶⁰, Konstantin Stankevich⁶⁹, Dušan Štefánek⁷⁰, Hans Steiger^{52,53}, Jochen Steinmann⁴⁸, Tobias Sterr⁵⁴, Matthias Raphael Stock⁵³, Virginia Strati⁵⁶, Alexander Studenikin⁶⁹, Shifeng Sun¹¹, Xilei Sun¹⁰, Yongjie Sun²², Yongzhao Sun¹⁰, Narumon Suwonjandee⁷¹, Michal Szelezniak⁴⁵, Jian Tang²⁰, Qiang Tang²⁰, Quan Tang²³,

Xiao Tang¹⁰, Alexander Tietzsch⁵⁴, Igor Tkachev⁶⁸, Tomas Tmej⁴¹, Marco Danilo Claudio Torri⁴¹, Konstantin Treskov⁶⁷, Andrea Triossi⁴⁵, Giancarlo Troni⁵, Wladyslaw Trzaska⁴², Cristina Tuve⁵⁵, Nikita Ushakov⁶⁸, Johannes van den Boom⁵¹, Stefan van Waasen⁵¹, Guillaume Vanroyen⁴⁷, Vadim Vedin⁶⁵, Giuseppe Verde⁵⁵, Maxim Vialkov⁶⁹, Benoit Viaud⁴⁷, Moritz Vollbrecht^{50,48}, Cristina Volpe⁴³, Vit Vorobel⁴¹, Dmitriy Voronin⁶⁸, Lucia Votano⁶³, Pablo Walker⁵, Caishen Wang¹⁸, Chung-Hsiang Wang³⁹, En Wang³⁷, Guoli Wang²¹, Jian Wang²², Jun Wang²⁰, Kunyu Wang¹⁰, Lu Wang¹⁰, Meifen Wang¹⁰, Meng Wang²³, Meng Wang²⁵, Rui Guang Wang¹⁰, Siguang Wang¹², Wei Wang²⁷, Wei Wang²⁰, Wenshuai Wang¹⁰, Xi Wang¹⁶, Xiangyue Wang²⁰, Yangfu Wang¹⁰, Yaoguang Wang¹⁰, Yi Wang¹³, Yi Wang²⁴, Yifang Wang¹⁰, Yuanqing Wang¹³, Yuman Wang²⁷, Zhe Wang¹³, Zheng Wang¹⁰, Zhimin Wang¹⁰, Zongyi Wang¹³, Muhammad Waqas⁶⁶, Apimook Watcharangkool⁷², Lianghong Wei¹⁰, Wei Wei¹⁰, Wenlu Wei¹⁰, Yadong Wei¹⁸, Kaile Wen¹⁰, Liangjian Wen¹⁰, Christopher Wiebusch⁴⁸, Steven Chan-Fai Wong²⁰, Bjoern Wonsak⁴⁹, Diru Wu¹⁰, Qun Wu²⁵, Zhi Wu¹⁰, Michael Wurm⁵², Jacques Wurtz⁴⁵, Christian Wysotzki⁴⁸, Yufei Xi³², Dongmei Xia¹⁷, Xiaochuan Xie¹⁷, Yuguang Xie¹⁰, Zhangquan Xie¹⁰, Zhizhong Xing¹⁰, Benda Xu¹³, Cheng Xu²³, Donglian Xu^{31,30}, Fanrong Xu¹⁹, Hangkun Xu¹⁰, Jilei Xu¹⁰, Jing Xu⁸, Meihang Xu¹⁰, Yin Xu³³, Yu Xu^{50,48}, Baojun Yan¹⁰, Taylor Yan⁷³, Wenqi Yan¹⁰, Xiongbo Yan¹⁰, Yupeng Yan⁷³, Anbo Yang¹⁰, Changgen Yang¹⁰, Chengfeng Yang²⁸, Huan Yang¹⁰, Jie Yang³⁷, Lei Yang¹⁸, Xiaoyu Yang¹⁰, Yifan Yang¹⁰, Yifan Yang², Haifeng Yao¹⁰, Zafar Yasin⁶⁶, Jiakuan Ye¹⁰, Mei Ye¹⁰, Ziping Ye³¹, Ugur Yegin⁵¹, Frédéric Yermia⁴⁷, Peihuai Yi¹⁰, Na Yin²⁵, Xiangwei Yin¹⁰, Zhengyun You²⁰, Boxiang Yu¹⁰, Chiye Yu¹⁸, Chunxu Yu³³, Hongzhao Yu²⁰, Miao Yu³⁴, Xianghui Yu³³, Zeyuan Yu¹⁰, Zezhong Yu¹⁰, Chengzhuo Yuan¹⁰, Ying Yuan¹², Zhenxiong Yuan¹³, Ziyi Yuan³⁴, Baobiao Yue²⁰, Noman Zafar⁶⁶, Andre Zambanini⁵¹, Vitalii Zavadskiy⁶⁷, Shan Zeng¹⁰, Tingxuan Zeng¹⁰, Yuda Zeng²⁰, Liang Zhan¹⁰, Aiqiang Zhang¹³, Feiyang Zhang³⁰, Guoqing Zhang¹⁰, Haiqiong Zhang¹⁰, Honghao Zhang²⁰, Jiawen Zhang¹⁰, Jie Zhang¹⁰, Jin Zhang²⁸, Jingbo Zhang²¹, Jinnan Zhang¹⁰, Peng Zhang¹⁰, Qingmin Zhang³⁵, Shiqi Zhang²⁰, Shu Zhang²⁰, Tao Zhang³⁰, Xiaomei Zhang¹⁰, Xuantong Zhang¹⁰, Xueyao Zhang²⁵, Yan Zhang¹⁰, Yinong Zhang¹⁰, Yiyu Zhang¹⁰, Yongpeng Zhang¹⁰, Yuanyuan Zhang³⁰, Yumei Zhang²⁰, Zhenyu Zhang³⁴, Zhijian Zhang¹⁸, Fengyi Zhao²⁶, Jie Zhao¹⁰, Rong Zhao²⁰, Shujun Zhao³⁷, Tianchi Zhao¹⁰, Dongqin Zheng¹⁹, Hua Zheng¹⁸, Minshan Zheng⁹, Yangheng Zheng¹⁴, Weirong Zhong¹⁹, Jing Zhou⁹, Li Zhou¹⁰, Nan Zhou²², Shun Zhou¹⁰, Tong Zhou¹⁰, Xiang Zhou³⁴, Jiang Zhu²⁰, Kangfu Zhu³⁵, Kejun Zhu¹⁰, Zhihang Zhu¹⁰, Bo Zhuang¹⁰, Honglin Zhuang¹⁰, Liang Zong¹³, and Jiaheng Zou¹⁰.

¹ Yerevan Physics Institute, Yerevan, Armenia.

² Université Libre de Bruxelles, Brussels, Belgium.

³ Universidade Estadual de Londrina, Londrina, Brazil.

⁴ Pontifícia Universidade Católica do Rio de Janeiro, Rio, Brazil.

⁵ Pontificia Universidad Católica de Chile, Santiago, Chile.

⁶ Universidad Técnica Federico Santa María, Valparaíso, Chile.

⁷ Beijing Institute of Spacecraft Environment Engineering, Beijing, China.

⁸ Beijing Normal University, Beijing, China.

⁹ China Institute of Atomic Energy, Beijing, China.

¹⁰ Institute of High Energy Physics, Beijing, China.

¹¹ North China Electric Power University, Beijing, China.

¹² School of Physics, Peking University, Beijing, China.

¹³ Tsinghua University, Beijing, China.

¹⁴ University of Chinese Academy of Sciences, Beijing, China.

¹⁵ Jilin University, Changchun, China.

¹⁶ College of Electronic Science and Engineering, National University of Defense Technology, Changsha, China.

¹⁷ Chongqing University, Chongqing, China.

¹⁸ Dongguan University of Technology, Dongguan, China.

¹⁹ Jinan University, Guangzhou, China.

²⁰ Sun Yat-Sen University, Guangzhou, China.

²¹ Harbin Institute of Technology, Harbin, China.

²² University of Science and Technology of China, Hefei, China.

²³ The Radiochemistry and Nuclear Chemistry Group in University of South China, Hengyang, China.

²⁴ Wuyi University, Jiangmen, China.

²⁵ Shandong University, Jinan, China, and Key Laboratory of Particle Physics and Particle Irradiation of Ministry of Education, Shandong University, Qingdao, China.

²⁶ Institute of Modern Physics, Chinese Academy of Sciences, Lanzhou, China.

²⁷ Nanjing University, Nanjing, China.

²⁸ Guangxi University, Nanning, China.

²⁹ East China University of Science and Technology, Shanghai, China.

³⁰ School of Physics and Astronomy, Shanghai Jiao Tong University, Shanghai, China.

³¹ Tsung-Dao Lee Institute, Shanghai Jiao Tong University, Shanghai, China.

³² Institute of Hydrogeology and Environmental Geology, Chinese Academy of Geological Sciences, Shijiazhuang, China.

³³ Nankai University, Tianjin, China.

³⁴ Wuhan University, Wuhan, China.

³⁵ Xi'an Jiaotong University, Xi'an, China.

³⁶ Xiamen University, Xiamen, China.

- 37 School of Physics and Microelectronics, Zhengzhou University, Zhengzhou, China.
- 38 Institute of Physics, National Yang Ming Chiao Tung University, Hsinchu.
- 39 National United University, Miao-Li.
- 40 Department of Physics, National Taiwan University, Taipei.
- 41 Charles University, Faculty of Mathematics and Physics, Prague, Czech Republic.
- 42 University of Jyväskylä, Department of Physics, Jyväskylä, Finland.
- 43 IJCLab, Université Paris-Saclay, CNRS/IN2P3, 91405 Orsay, France.
- 44 Univ. Bordeaux, CNRS, CENBG, UMR 5797, F-33170 Gradignan, France.
- 45 IPHC, Université de Strasbourg, CNRS/IN2P3, F-67037 Strasbourg, France.
- 46 Centre de Physique des Particules de Marseille, Marseille, France.
- 47 SUBATECH, Université de Nantes, IMT Atlantique, CNRS-IN2P3, Nantes, France.
- 48 III. Physikalisches Institut B, RWTH Aachen University, Aachen, Germany.
- 49 Institute of Experimental Physics, University of Hamburg, Hamburg, Germany.
- 50 Forschungszentrum Jülich GmbH, Nuclear Physics Institute IKP-2, Jülich, Germany.
- 51 Forschungszentrum Jülich GmbH, Central Institute of Engineering, Electronics and Analytics - Electronic Systems (ZEA-2), Jülich, Germany.
- 52 Institute of Physics, Johannes-Gutenberg Universität Mainz, Mainz, Germany.
- 53 Technische Universität München, München, Germany.
- 54 Eberhard Karls Universität Tübingen, Physikalisches Institut, Tübingen, Germany.
- 55 INFN Catania and Dipartimento di Fisica e Astronomia dell'Università di Catania, Catania, Italy.
- 56 Department of Physics and Earth Science, University of Ferrara and INFN Sezione di Ferrara, Ferrara, Italy.
- 57 INFN Sezione di Milano and Dipartimento di Fisica dell'Università di Milano, Milano, Italy.
- 58 INFN Milano Bicocca and University of Milano Bicocca, Milano, Italy.
- 59 INFN Milano Bicocca and Politecnico di Milano, Milano, Italy.
- 60 INFN Sezione di Padova, Padova, Italy.
- 61 Dipartimento di Fisica e Astronomia dell'Università di Padova and INFN Sezione di Padova, Padova, Italy.
- 62 INFN Sezione di Perugia and Dipartimento di Chimica, Biologia e Biotecnologie dell'Università di Perugia, Perugia, Italy.
- 63 Laboratori Nazionali di Frascati dell'INFN, Roma, Italy.
- 64 University of Roma Tre and INFN Sezione Roma Tre, Roma, Italy.
- 65 Institute of Electronics and Computer Science, Riga, Latvia.
- 66 Pakistan Institute of Nuclear Science and Technology, Islamabad, Pakistan.
- 67 Joint Institute for Nuclear Research, Dubna, Russia.
- 68 Institute for Nuclear Research of the Russian Academy of Sciences, Moscow, Russia.
- 69 Lomonosov Moscow State University, Moscow, Russia.
- 70 Comenius University Bratislava, Faculty of Mathematics, Physics and Informatics, Bratislava, Slovakia.
- 71 Department of Physics, Faculty of Science, Chulalongkorn University, Bangkok, Thailand.
- 72 National Astronomical Research Institute of Thailand, Chiang Mai, Thailand.
- 73 Suranaree University of Technology, Nakhon Ratchasima, Thailand.
- 74 Department of Physics and Astronomy, University of California, Irvine, California, USA.